Electronic Supplementary Information

Modelling the elusive conformational activation in kynurenine 3-monooxygenase

Yılmaz Özkılıç[†,] and Matthias Stein[†]*

[†]Molecular Simulations and Design Group, Max Planck Institute for Dynamics of Complex Technical Systems, Sandtorstrasse 1,39106 Magdeburg, Germany

*E-mail: ozkilic@mpi-magdeburg.mpg.de

Contents

Validation of the Quality of Protein Models

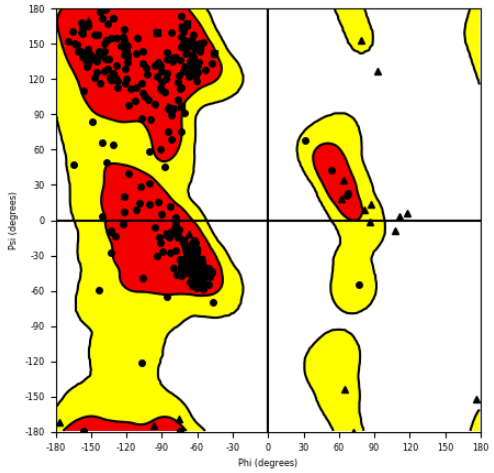

Fig. S1. Ramachandran plot of apo-KMO.

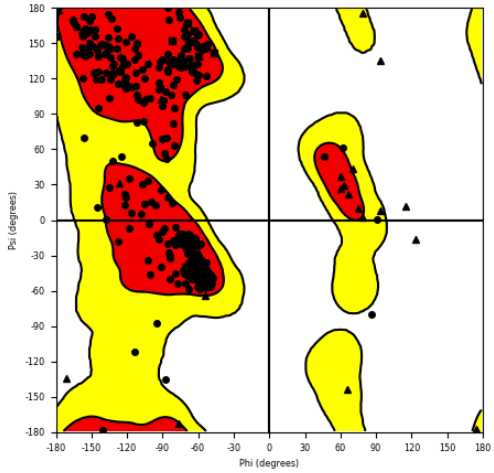

Fig. S2. Ramachandran plot of Inh_E–KMO.

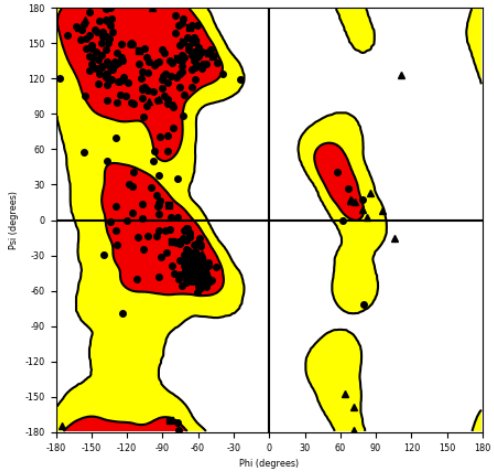

Fig. S3. Ramachandran plot of Inh_C–KMO.

Monitoring of MD Equilibration

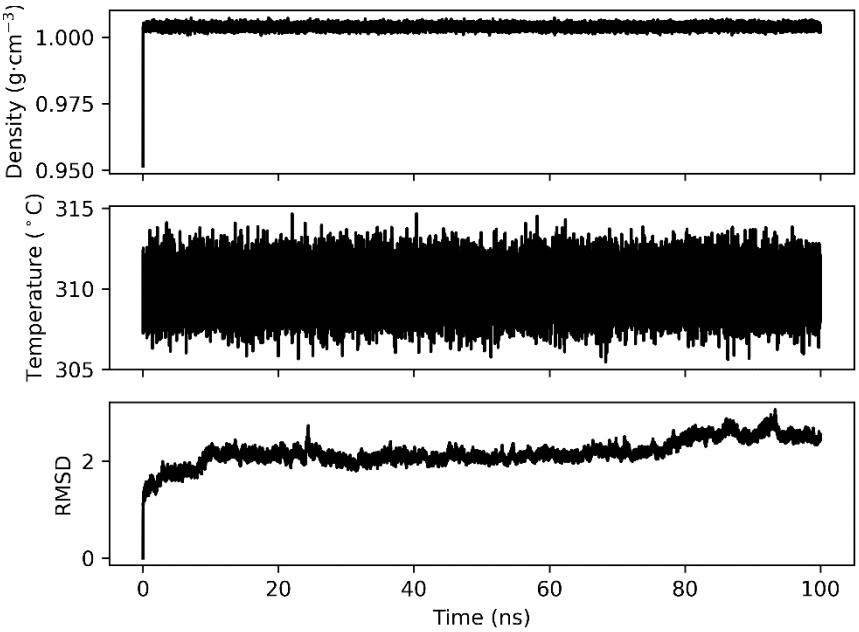

Fig. S4. Equilibration plots of apo-KMO.

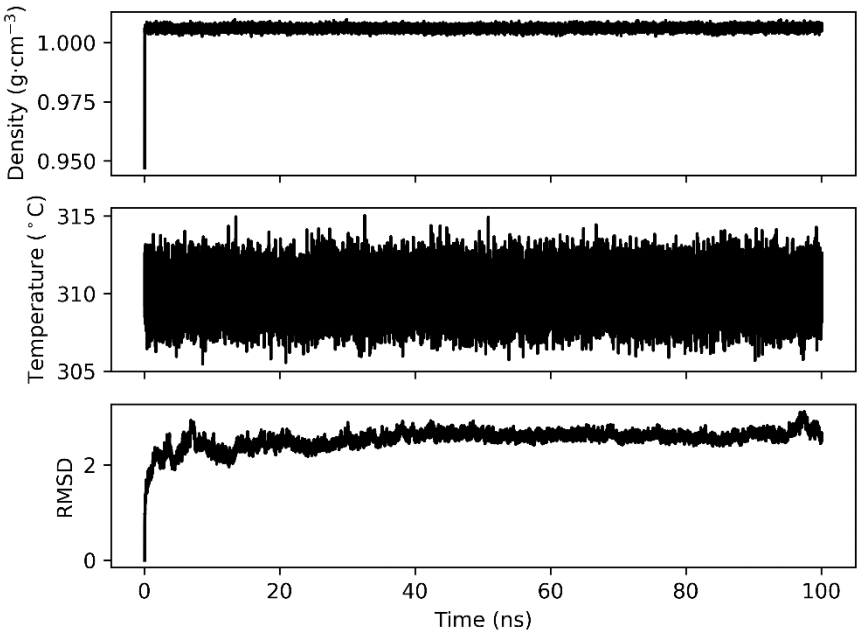

Fig. S5. Equilibration plots of Inh_E–KMO.

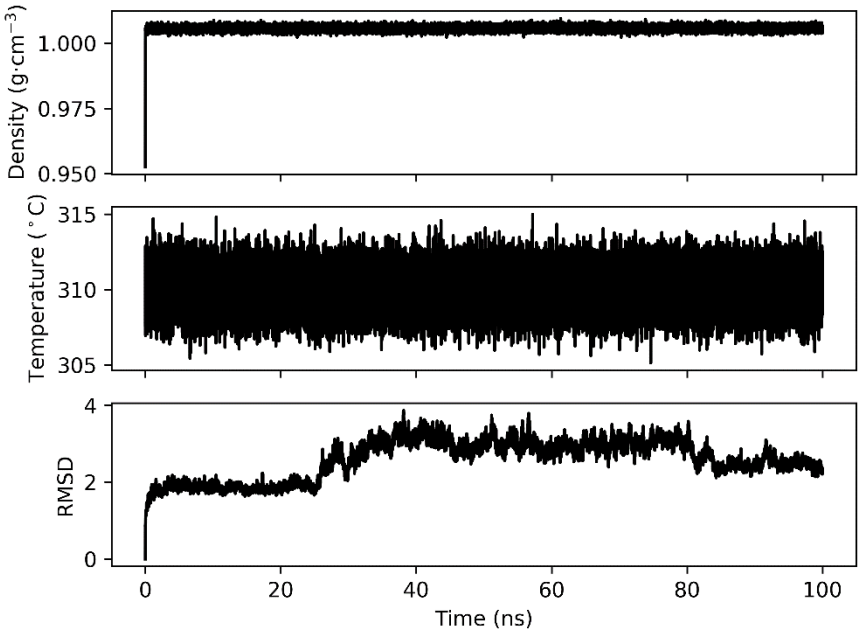

Fig. S6. Equilibration plots of Inh_C–KMO.

Verification of US Overlapping of Selected Windows

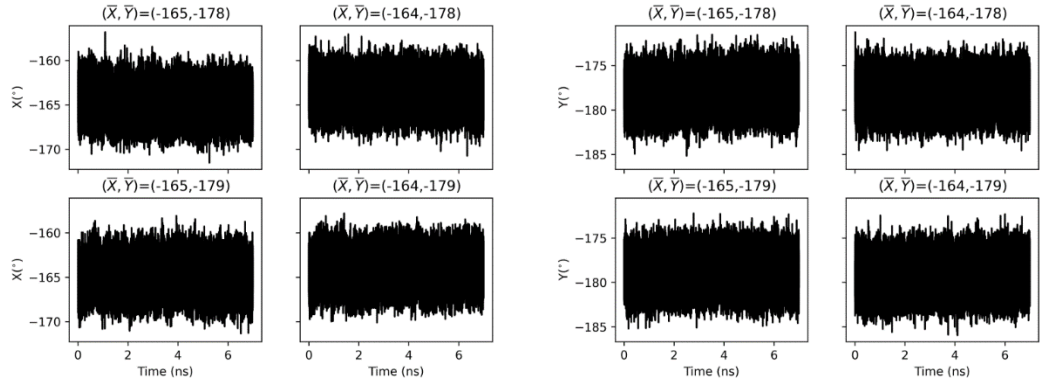

Fig. S7. Overlapping in both X (left) and Y (right) directions of the four trajectory files that span the *in* conformational state of apo-KMO. The variables with overbars indicate the central coordinates of the harmonic potential.

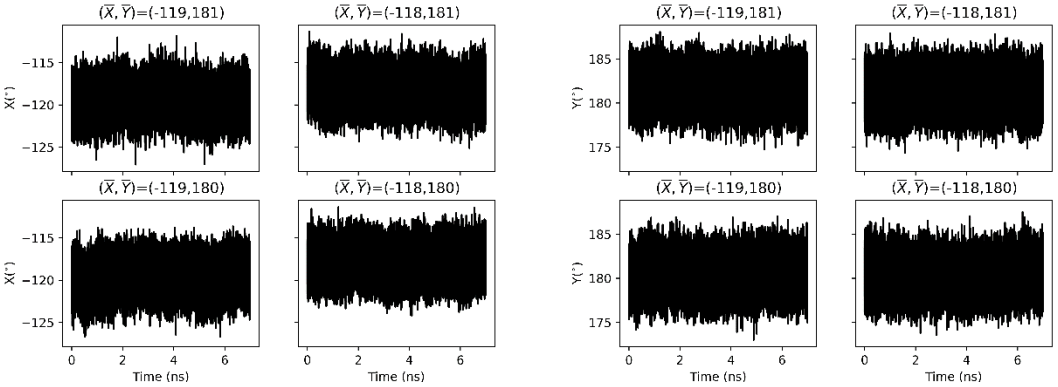

Fig. S8. Overlapping in both X (left) and Y (right) directions of the four trajectory files that span the TS of apo-KMO. The variables with overbars indicate the central coordinates of the harmonic potential.

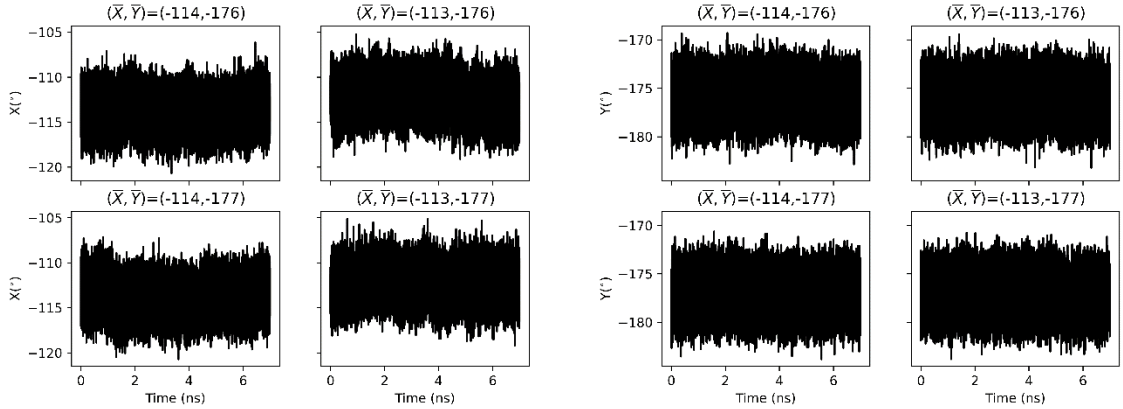

Fig. S9. Overlapping in both X (left) and Y (right) directions of the four trajectory files that span the *out* conformational state of apo-KMO. The variables with overbars indicate the central coordinates of the harmonic potential.

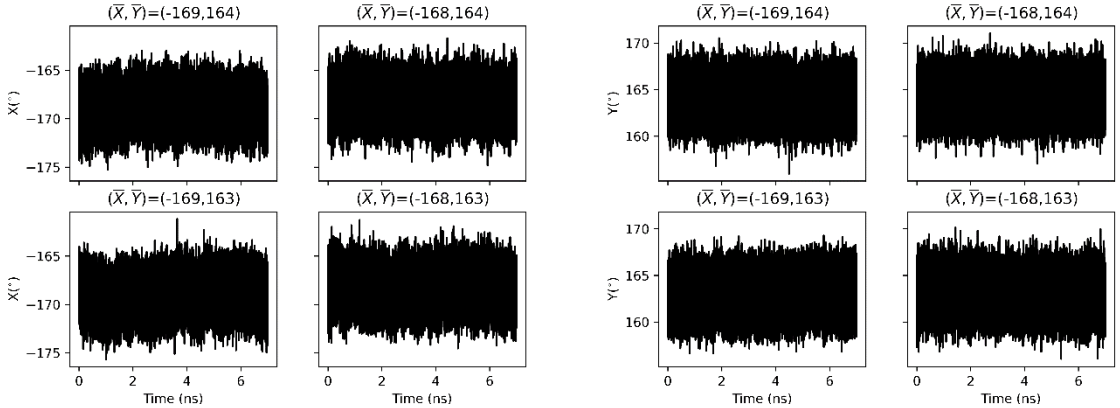

Fig. S10. Overlapping in both X (left) and Y (right) directions of the four trajectory files that span the *in* conformational state of Inh_E–KMO. The variables with overbars indicate the central coordinates of the harmonic potential.

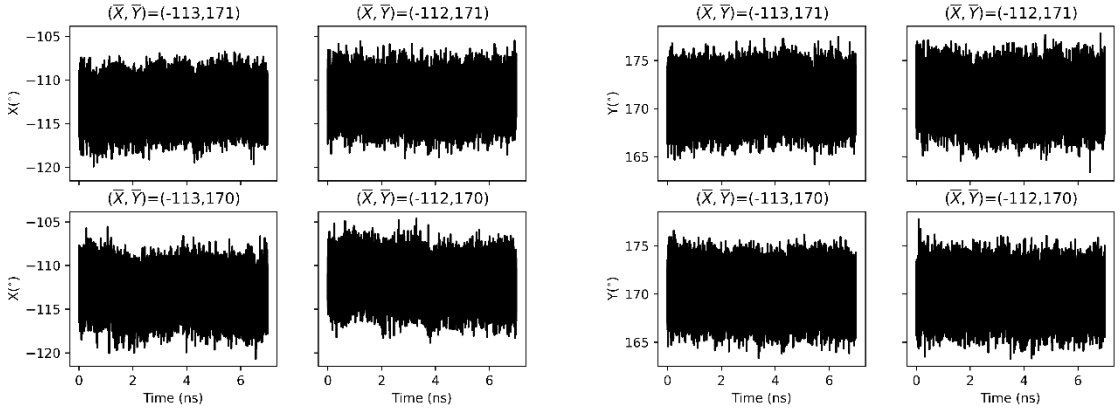

Fig. S11. Overlapping in both X (left) and Y (right) directions of the four trajectory files that span the TS of Inh_E–KMO. The variables with overbars indicate the central coordinates of the harmonic potential.

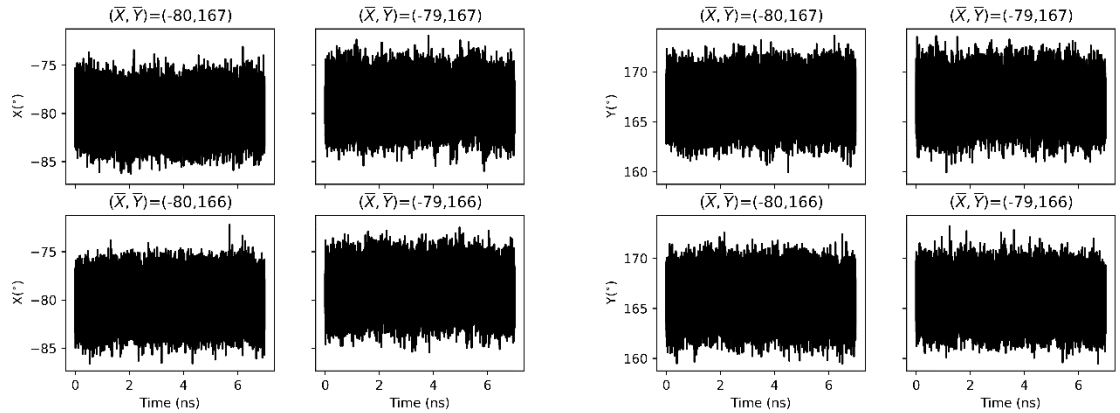

Fig. S12. Overlapping in both X (left) and Y (right) directions of the four trajectory files that span the *out* conformational state of Inh_E–KMO. The variables with overbars indicate the central coordinates of the harmonic potential.

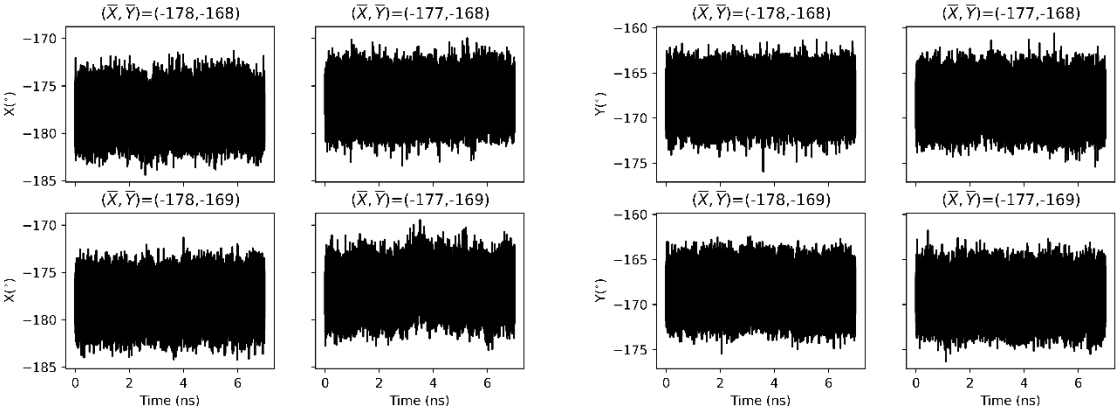

Fig. S13. Overlapping in both X (left) and Y (right) directions of the four trajectory files that span the *in* conformational state of Inh_C–KMO. The variables with overbars indicate the central coordinates of the harmonic potential.

Additional Free Energy Contour Maps for KMO Activation

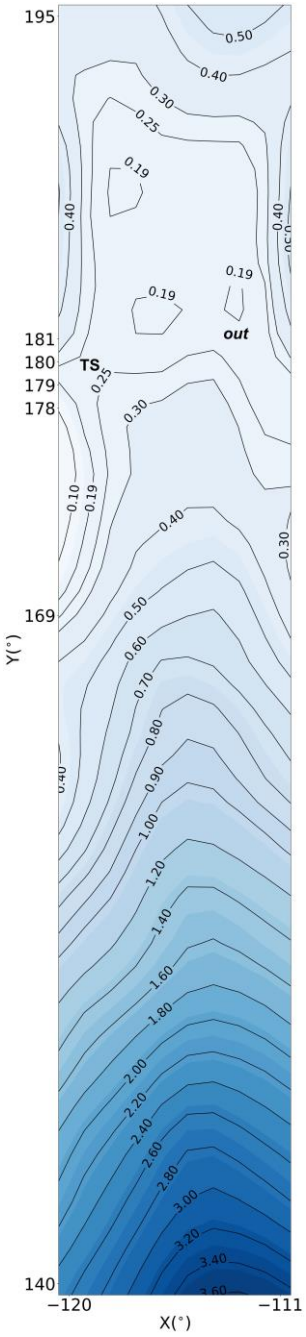

Fig. S14. Free energy contour map of apo-KMO. The contour was generated using the coordinates obtained from the slow US(X,145) run. Using ten coordinate points (X= [-120°, -111°] at Y=145°) ten slow US(Y) simulations were carried out in both decreasing (until Y=140°) and increasing (until Y=195°) directions in which X-angle is a parameter. The total production runtime is 3920 (10x56x7) ns. The numbers in the contour lines are relative free energy values but only within this range. The saddle point is located between X= [-118°, -119°] and Y= [180°, 181°]. The *out* conformational state is located between X= [-114°, -113°] and Y= [183°, 184°].

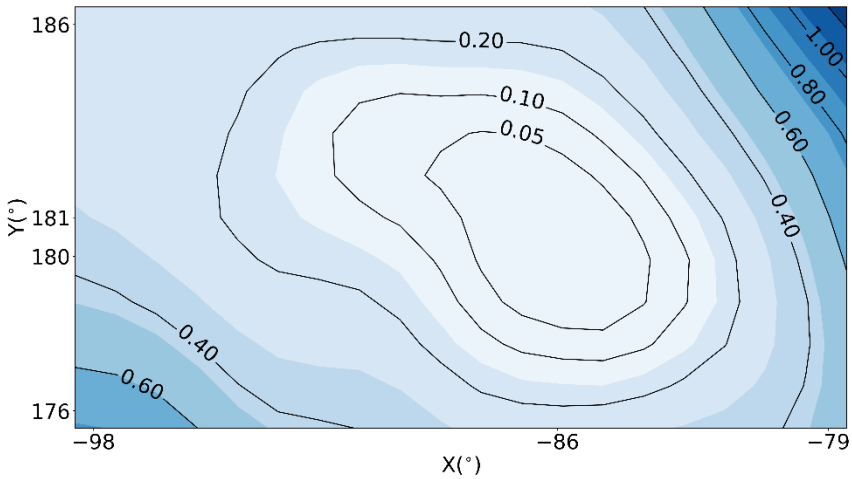

Fig. S15. The contour map was obtained using the coordinates obtained from the slow US(X) run shown in Fig. 5 for apo-KMO. Using these coordinate points (X=[-98°, -79°], Y=-179°) twenty slow US(Y) simulations were carried out in both decreasing (until Y=176°) and increasing (until Y=186°) directions in which X-angle is a parameter. The total production time is 1540(20x11x7) ns.

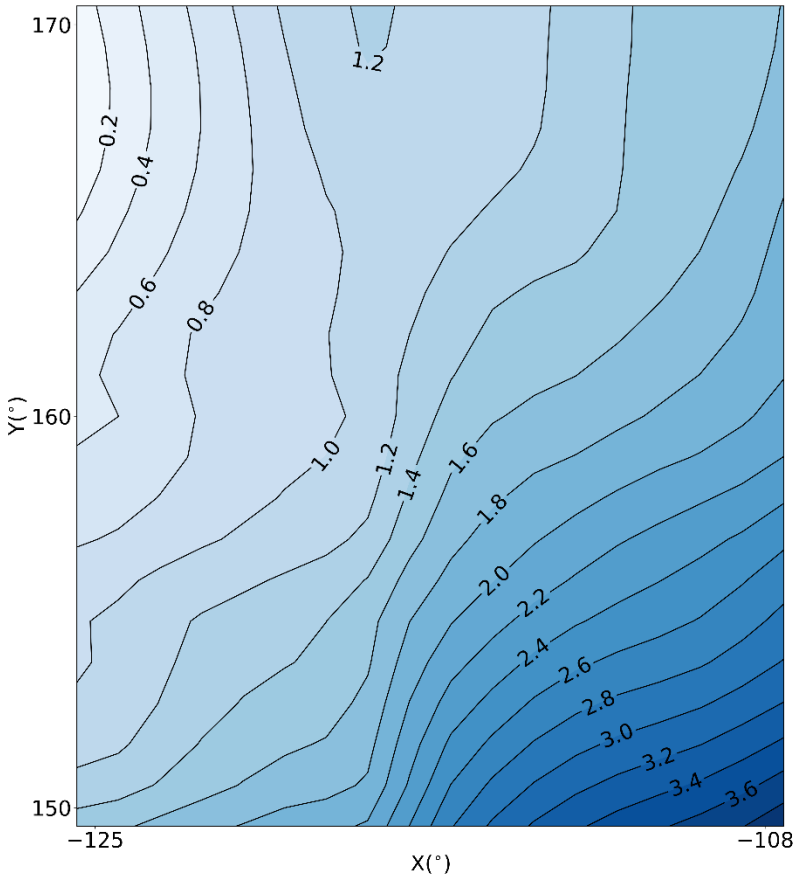

Fig. S16. The contour map was obtained using the coordinates obtained from the slow US(X,155) of the Inh_E–KMO. Using these coordinate points (X=[-125°, -108°], Y=155°) eighteen slow US(Y) simulations were carried out in both decreasing (until Y=150°) and increasing (until Y=170°) directions in which X-angle is a parameter. The total production time is 2646 (18x21x7) ns.

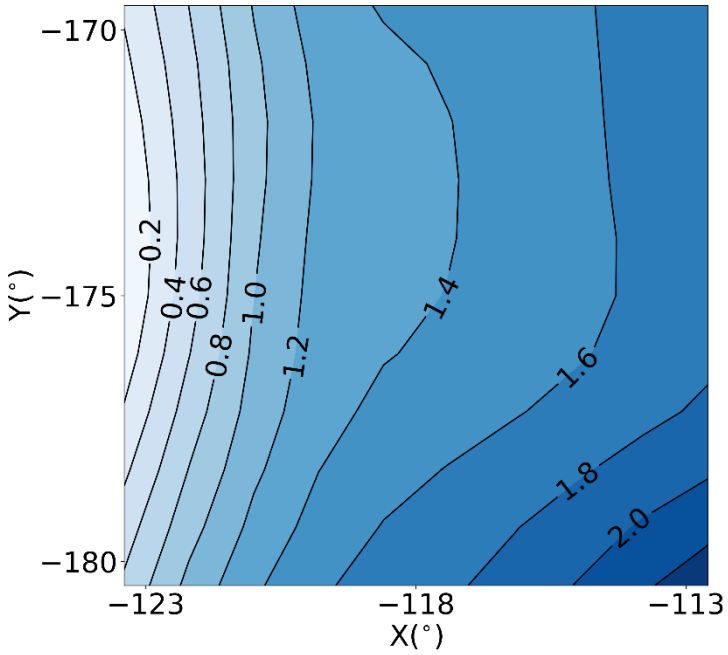

Fig. S17. The contour map was obtained using the coordinates obtained from the slow US(X, -175) of the Inh_C–KMO. Using these coordinate points (X=[-123°, -114°], Y=-175°) ten slow US(Y) simulations were carried out in both decreasing (until Y=180°) and increasing (until Y=-170°) directions in which X-angle is a parameter. The total production time is 770 (10x11x7) ns.

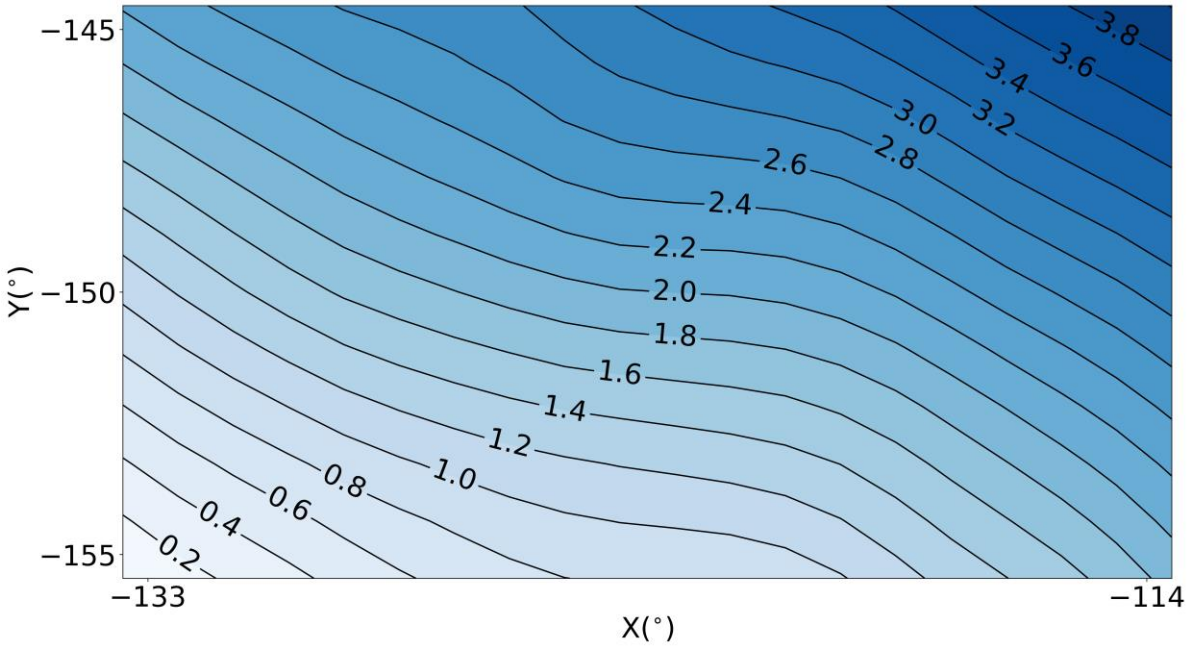

Fig. S18. The contour map was obtained using the coordinates obtained from the slow US(X, -150) of the Inh_C–KMO. Using these coordinate points (X=[-133°, -114°], Y=-150°) twenty slow US(Y) simulations were carried out in both decreasing (until Y= -155°) and increasing (until Y=-145°) directions in which X-angle is a parameter. The total production time is 1540 (20x11x7) ns.

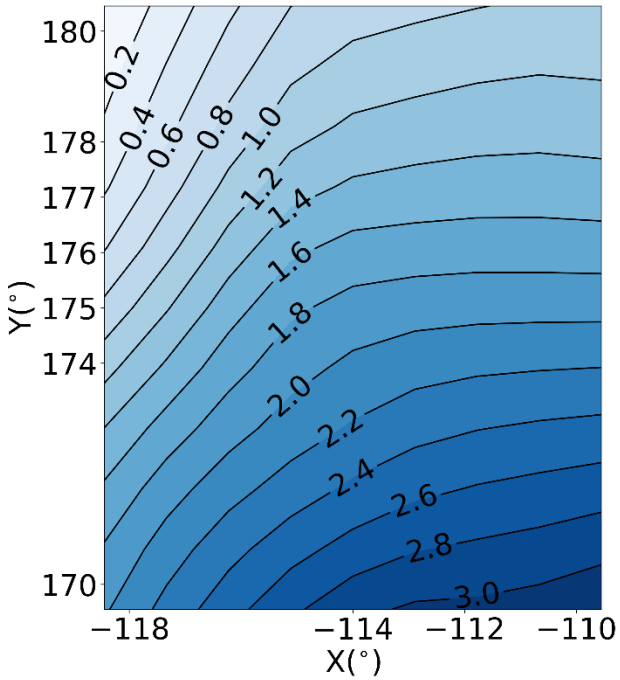

Fig. S19. The contour map was obtained using the coordinates obtained from the slow US(X, 175) of the Inh_C–KMO. Using these coordinate points (X=[-118°, -110°], Y=175°) nine slow US(Y) simulations were carried out in both decreasing (until Y=170°) and increasing (until Y=180°) directions in which X-angle is a parameter. The total production time is 693 (9x11x7) ns.

Details of Relative Free Energy Calculations of KMO Conformational States

Apo-KMO

(1) The global minimum of the *in* state (Fig. 6) can be considered at (X, Y)=(-164°, 180°). This is the minimum point of the slow US(X,180) as well. **(2)** Relative free energy of the point (X, Y) = (-175°, 180°) in the slow US(X,180) is +1.6 kcal/mol. **(3)** The minimum of the slow US(-175, Y) is at (-175°, 180°) and therefore, 1.6 kcal/mol above the global minimum. **(4)** The minimum of the slow US(X, 145) is at (-172°, 145°), and the relative free energy at (-175°, 145) (in this run) is +0.1 kcal/mol. **(5)** The relative free energy of the point (-175°, 145) in the slow US(-175,Y) is +6.4 kcal/mol. **(6)** It is understood from (3), (4) and (5) that the relative free energy of the point (-172°, 145°) is +7.9 (1.6-0.1+6.4) kcal/mol above the global minimum. **(7)** The relative free energy of the point (-115°, 145°) in the slow US(X, 145) is 11.3 kcal/mol. **(8)** The free energy of the point (-115°, 145°) in the free energy contour (Fig. S14) is 2.6 kcal/mol higher in comparison to the saddle point. **(9)** It is understood from (6), (7) and (8) that the free energy barrier of the *in* to the *out* state change is 16.6 (7.9+11.3-2.6) kcal/mol.

Inh_E–KMO

(1) The minimum of the slow US(X,170) in Fig. 9 is at (-162°, 170°) and is 0.5 kcal/mol higher in comparison to the global minimum (Fig. 10). **(2)** The free energy at the point (-113°, 170°) of the slow US(X,170) is 7.9 kcal/mol, and the saddle point in Fig. 10 is also at this point. Using the relative free energy (7.9 kcal/mol) of this point in the slow US(X,170), the barrier height is computed: 8.4 (7.9+0.5) kcal/mol. **(3)** The local minimum (-79, 170) in the slow US(X, 170) is at 4.6 kcal/mol. The contour minimum at (-79, 167) (‘*out’* in Fig. 10) is 0.1 kcal/mol lower in comparison to the local minimum of the slow US(X, 170). Therefore, the free energy change accompanying the conformational change is 5.0 (4.6+0.5-0.1) kcal/mol.

Structural Details of KMO Activation

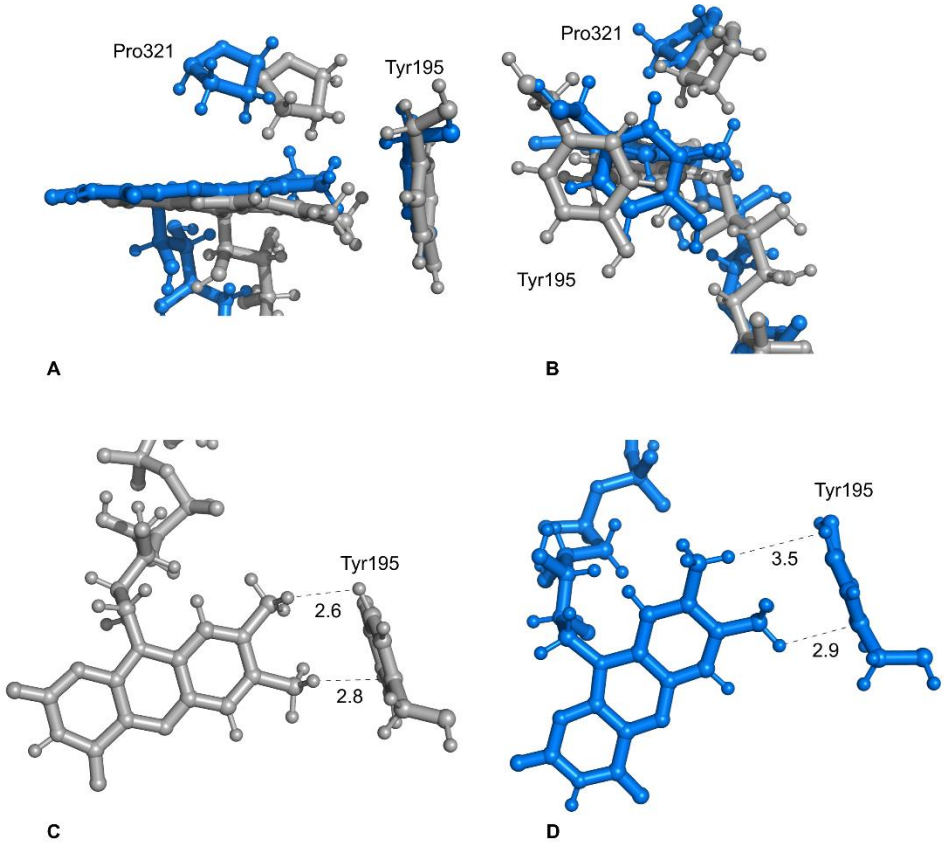

Fig. S20. A. Superposition TSs of (grey) apo-KMO and (blue) Inh_E–KMO. **B.** The same as in A but from a different viewpoint. **C.** Isoalloxazine–Tyr195 distances (one H–H and one C–H) in apo-KMO. **D.** Isoalloxazine–Tyr195 distances (one H–H and one C–H) in Inh_E–KMO.

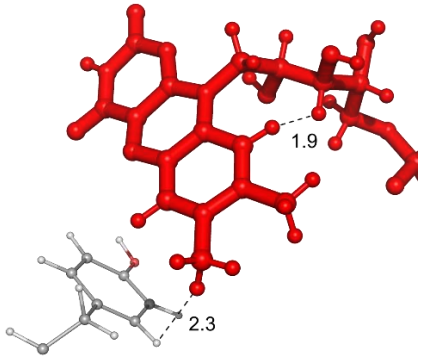

Fig. S21. The repelling H–H interactions in the *out* conformational state of apo-KMO

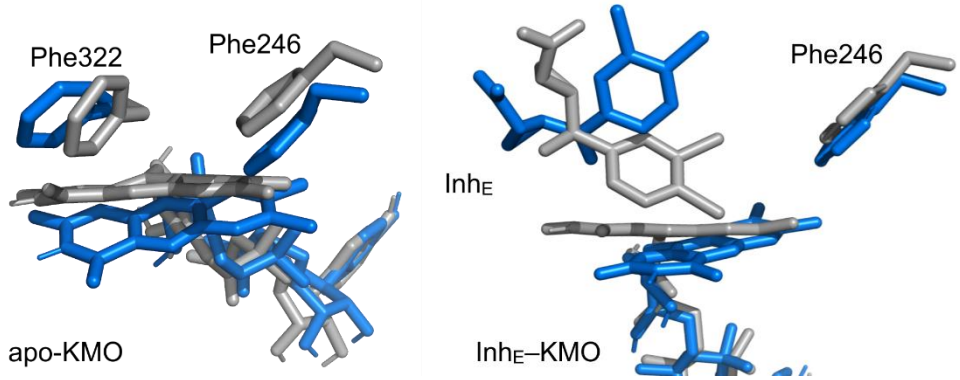

Fig. S22. Superposition of the *in* conformational state and the TS in apo-KMO and Inh_E–KMO. Interactions between Phe332 and Phe246 in the (grey) *in* conformational state and (blue) TS of apo-KMO, and between Inh_E and Phe246 in (grey) *in* conformational state and (blue) TS of Inh_E–KMO.

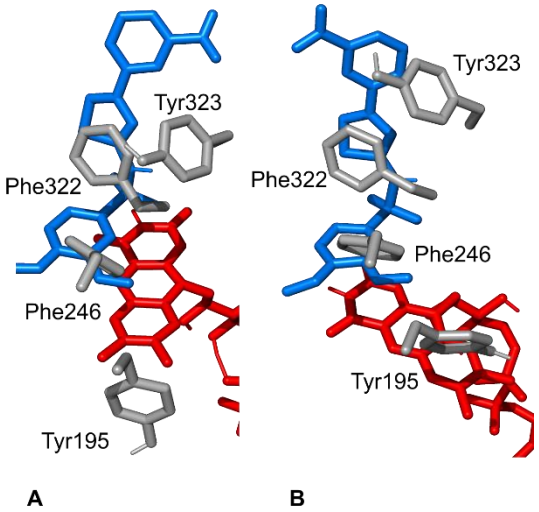

Fig. S23. A. Interactions between (blue) Inh_C and surrounding residues, and between Inh_C and (red) isoalloxazine in the *in* conformational state of Inh_C–KMO. (**B**) The same interactions in the high energy state that is defined in Fig. 17.

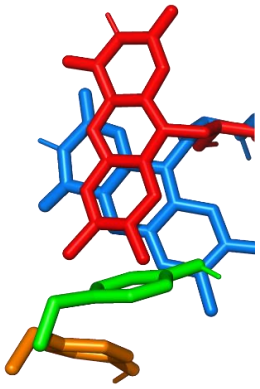

Fig. S24. Superposition of the *in* conformational state and high energy state that is defined in Fig. 17 of Inh_C–KMO displaying the displacement of (green) side chain of Tyr195 and (blue) isoalloxazine relative to their original positions (shown in orange and red, respectively).

Analysis of Number of Water Molecules Around the Isoalloxazine

In Table S1, the number of water molecules surrounding each polar atom of the isoalloxazine are reported. The numbers are rounded to the nearest integers. The first number indicates the number of water molecules within a sphere of 2.5 Å radius (which is surrounding the atom), and the second number indicates that of 3.5 Å radius. The numbers were obtained by averaging over the four trajectory files that are stated in caption of the free energy contour maps for each state.

Table S1. The number of water molecules surrounding each polar atom of the isoalloxazine in the ranges of 2.5 Å and 3.5 Å radii in various states of each protein complex.

Complex	Atomic label	***in* state**		**TS**		***out* state**	
		2.5 Å	3.5 Å	2.5 Å	3.5 Å	2.5 Å	3.5 Å
Apo-KMO	N1	0	1	0	1	1	2
	O2	0	0	0	1	1	2
	H3	1	1	0	1	1	2
	O4	1	3	1	1	2	3
	N5	1	2	1	2	0	1
Inh_E–KMO	N1	0	0	1	2	1	2
	O2	0	0	1	2	2	5
	H3	0	0	1	1	1	3
	O4	0	1	1	2	1	2
	N5	1	1	0	1	0	1
Inh_C–KMO	N1	0	1				
	O2	0	0				
	H3	0	0				
	O4	0	1				
	N5	0	1				